Serotonergic modulation of hyperpolarization-activated current in acutely isolated rat dorsal root ganglion neurons

Carla G. Cardenas, Lucinda P. Del Mar, Alexander V. Vysokanov, Peter B. Arnold, Luz M. Cardenas, D. James Surmeier* and Reese S. Scroggs

*Department of Anatomy and Neurobiology, College of Medicine, University of Tennessee, Memphis, TN 38163 and *Department of Physiology, Northwestern University Medical School, Chicago, IL 60611, USA*

(Received 4 January 1999; accepted after revision 15 April 1999)

1. The effect of serotonin (5-HT) on the hyperpolarization-activated cation current (I_H) was studied in small-, medium- and large-diameter acutely isolated rat dorsal root ganglion (DRG) cells, including cells categorized as type 1, 2, 3 and 4 based on membrane properties. 5-HT increased I_H in 91 % of medium-diameter DRG cells (including type 4) and in 67 % of large-diameter DRG cells, but not other DRG cell types.

2. The increase of I_H by 5-HT was antagonized by spiperone but not cyanopindolol, and was mimicked by 5-carboxyamidotryptamine, but not (+)-8-hydroxydipropylaminotetralin (8-OH-DPAT) or cyanopindolol. These data suggested the involvement of 5-HT_7 receptors, which were shown to be expressed by medium-diameter DRG cells using RT-PCR analysis.

3. 5-HT shifted the conductance–voltage relationship of I_H by +6 mV without changing peak conductance. The effects of 5-HT on I_H were mimicked and occluded by forskolin, but not by inactive 1,9-dideoxy forskolin.

4. At holding potentials negative to −50 mV, 5-HT increased steady-state inward current and instantaneous membrane conductance (fast current). The 5-HT-induced inward current and fast current were blocked by Cs^+ but not Ba^{2+} and reversed at −23 mV, consistent with the properties of tonically activated I_H.

5. In medium-diameter neurons recorded from in the current clamp mode, 5-HT depolarized the resting membrane potential, decreased input resistance and facilitated action potential generation by anode-break excitation.

6. The above data suggest that in distinct subpopulations of DRG neurons, 5-HT increases cAMP levels via activation of 5-HT_7 receptors, which shifts the voltage dependence of I_H to more depolarized potentials and increases neuronal excitability.

The hyperpolarization-activated cation current (I_H) is expressed differentially in various subpopulations of rat sensory neurons. For example, I_H is infrequently expressed by C- and Aδ-type dorsal root ganglion (DRG) neurons but is prominent in most Aα- and Aβ-type DRG neurons (Harper & Lawson, 1985*a*,*b*; Scroggs *et al.* 1994; Valiere & McLachlan, 1996). Since C- and Aδ-type DRG neurons are typically involved in the transmission of different types of information than Aβ- and Aα-type DRG neurons, it is likely that agents which modulate I_H may selectively affect certain types of sensory information. Serotonin (5-HT) has previously been shown to increase I_H in rat nucleus prepositus hypoglossi neurons and in guinea-pig thalamic neurons through an increase in cAMP. However, the possibility that 5-HT may modulate I_H in DRG neurons, as well as the potential mechanisms involved, have not previously been explored.

In an earlier study we developed a set of criteria which appeared useful in categorizing small- and medium-diameter DRG cell bodies into four groups, types 1, 2, 3 and 4, based on capsaicin sensitivity, expression of I_H, I_A (a transient, 4-aminopyridine-sensitive outward K^+ current) and T-type Ca^{2+} current amplitude (Cardenas *et al.* 1995). The likelihood that these categories have some functional significance is supported by subsequent findings that 5-HT_{1A} receptor activation selectively inhibited high-threshold Ca^{2+} currents in type 1 DRG cells and 5-HT_4 receptor activation selectively increased TTX-insensitive Na^+ currents in type 2 DRG cells (Cardenas *et al.* 1995, 1997*a*,*b*).

In the present study we observed that 5-HT increased I_H in type 4 DRG cells and a subpopulation of large-diameter DRG cells, but not in type 1, 2, or 3 DRG cells. The 5-HT receptor involved responded to several selective 5-HT

receptor ligands with a pattern similar to the 5-HT receptor that couples to I_H in rat prepositus hypoglossi neurons, and which is consistent with the pharmacological profile of the 5-HT_7 receptor. In addition, studies with the adenylyl cyclase activator forskolin suggest that the effect of 5-HT on I_H in DRG cells may involve an increase in cAMP.

These data suggest that 5-HT secreted into the spinal cord or into injured tissues may modulate excitability and firing patterns in certain functionally distinct subpopulations of sensory neurons via changes in I_H. 5-HT-induced changes in I_H could possibly be involved in the modulation of neurotransmitter release, the sensitivity of peripheral sensory receptors and the ectopic spontaneous discharges of DRG cells associated with peripheral nerve injury.

METHODS

Male rats (50–150 g, Sprague–Dawley, Harlan) were rendered unconscious by inhalation of methoxyflurane and decapitated, and DRGs from the thoracic and lumbar regions were dissected out. All procedures were approved by the University of Tennessee, Memphis Animal Care and Use Committee. The ganglia were incubated at 36 °C for 1 h in Tyrode solution (composition below) containing 2 mg ml^{-1} collagenase (Sigma, Type 1) and 5 mg ml^{-1} Dipase II (Boehringer-Mannheim). Individual DRG cell bodies were isolated by trituration, adhered to the bottom of a 35 mm Petri dish and superfused with Tyrode solution containing (mM): 140 NaCl, 4 KCl, 2 $MgCl_2$, 2 $CaCl_2$, 10 glucose and 10 Hepes, adjusted to pH 7·4 with NaOH. Recordings were obtained from the DRG cells within 10 min to 3 h of plating. Current and voltage were recorded in the whole-cell patch configuration using an Axopatch 200A (Axon Instruments). Voltage and current steps, holding potential, data acquisition and data analysis were controlled by an on-line IBM PC/AT clone computer programmed with Axobasic 1.0 (Axon Instruments).

Electrodes were fabricated from soda lime capillary glass (Scientific Products, B4416-1) using a Narishige 2-stage vertical puller, coated with Sylgard to about 200 μm from the tip and fire polished to a final resistance of 0·8–2·0 MΩ, using a Narishige microforge. For voltage clamp experiments, series resistance was estimated from capacity transients and compensated for as described previously (Scroggs & Fox, 1992). No data were included where series resistance resulted in greater than a 10 mV error in voltage commands.

DRG cell bodies under study were individually superfused with solutions using a glass capillary tube mounted on a micromanipulator. The end of the glass capillary tube was placed near the cell under study and the flow from it completely isolated the cell from the background flow of Tyrode solution, which continuously flowed over the cells via another port. Different solutions were directed out of the capillary tube by means of a small manifold to which various 10 ml aliquots of drug or control solutions were connected. Changes in appropriate ion currents produced by switching from Tyrode solution to solutions containing TEA, Ba^{2+}, Cs^+, Cd^{2+} or elevated K^+ indicated that the solution surrounding the cell under study was changed in less than 4 s by this system. All experiments were done at room temperature (23 °C).

Capsaicin (Sigma), forskolin and 1,9-dideoxy forskolin (RBI) were dissolved in 100% ethanol at a concentration of 10 mM (capsaicin) or 100 mM (forskolin) and diluted to 1 or 10 μM in Tyrode solution for experiments. Control experiments determined that the ethanol vehicle (0·1%) had no effect by itself on holding current or membrane conductance in capsaicin-sensitive DRG cells. Serotonin (5-HT), (+)-8-hydroxydipropylaminotetralin (8-OH-DPAT), 5-carboxyamido-tryptamine (5-CT) and (±)cyanopindolol (RBI) were first dissolved in water as 1 or 10 mM stock solutions and then diluted to appropriate concentrations in Tyrode solution for experiments. Spiperone (RBI) was first dissolved in 100% dimethylsulphoxide at a concentration of 10 mM and diluted to 1 μM in Tyrode solution for the experiments.

For some experiments, DRG cells were categorized as type 1, 2, 3 or 4 based on the expression of several membrane properties (capsaicin sensitivity, I_H, I_A and T-type Ca^{2+} channel current amplitude), as described previously (Cardenas *et al.* 1995) and illustrated in Fig. 1*A*. Each DRG cell was initially tested for I_H (a slowly activating non-selective cation current activated by hyperpolarization) using a 787 ms hyperpolarizing test pulse to −110 mV from a holding potential of −50 mV (Fig. 1*Bc*). A subtype of I_A (a group of transient, 4-aminopyridine-sensitive, outward K^+ currents; see Gold *et al.* 1996) was subsequently tested for upon repolarization of the DRG cell back to the holding potential (−50 mV) from the −110 mV test pulse used to test for I_H (Cardenas *et al.* 1995) (Fig. 1*Bc*). Next, cells were tested for capsaicin sensitivity by superfusion with 1 μM capsaicin, which produced an inward shift in holding current and an increase in membrane conductance in sensitive cells (Fig. 1*Bd*). Capsaicin-insensitive cells were subsequently tested for T-type Ca^{2+} channel current amplitude at a holding potential of −90 mV and a 200 ms test potential to −30 mV (Fig. 1*Bf*). Capsaicin-sensitive DRG cells without I_H or I_A were designated type 1 (Fig. 1*A*). Capsaicin-sensitive DRG cells expressing I_A were designated type 2 (Fig. 1*A*). Capsaicin-insensitive DRG cells that expressed I_H but not I_A and had small T-type Ca^{2+} channel currents (< 1 nA) were designated type 3 (Fig. 1*A*). Capsaicin-insensitive DRG cells that expressed I_H but not I_A and had large T-type Ca^{2+} channel currents (> 2 nA) were designated type 4 (Fig. 1*A*). In addition to the membrane properties used to categorize small- and medium-diameter DRG cells as type 1, 2, 3 or 4, Fig. 1*B* also illustrates the characteristic action potential shapes, TTX-sensitive and -insensitive Na^+ currents, L- and N-type high-threshold Ca^{2+} currents, expression of an inwardly rectifying current (I_{IR}) and a lactoseries carbohydrate surface antigen (Galβ1-4 GlcNAc-R), and cell diameter, all of which vary significantly among DRG cell types 1, 2, 3 and 4 (Cardenas *et al.* 1995, 1997*a*; Del Mar & Scroggs, 1996).

The present study also included large-diameter DRG neurons (⩾ 45 μm in diameter) and medium-diameter DRG neurons (31·3–40 μm in diameter) which were not characterized. Previous studies have indicated that nearly all medium-diameter DRG cells with smooth membrane surfaces free of satellite cells fit the type 4 category. In addition, some small-diameter DRG neurons (15–30 μm in diameter), which did not fit into the type 1, 2, 3 or 4 categories, were included in the study (see Fig. 1*A*). In our laboratory, whole-cell patch recordings are routinely obtained from DRG cells which have a smooth cell membrane that is free of adhering satellite cells. However, in our acutely dissociated preparations there are numerous DRG cells in all size ranges which have a rough appearance, probably due to the presence of satellite cells adhering to the cell membrane. At present we do not know whether or not these 'rough' DRG cells have different membrane properties to the cells we routinely recorded from.

For most experiments, DRG cells were superfused with Tyrode solution externally and the patch electrodes were filled with (mM): 150 potassium aspartate, 5 Na_2-ATP, 0·4 Na_2-GTP, 5 EGTA, 1·83

$CaCl_2$ and 20 Hepes, adjusted to pH 7·4 with Hepes. Free $[Ca^{2+}]_i$ was calculated at 100 nM. In some experiments Ca^{2+} channel currents (carried by Ba^{2+}) were isolated by changing the Tyrode solution superfusing the outside of the DRG cell under study to a solution containing (mM): 160 TEA-Cl, 2 $BaCl_2$ and 10 Hepes, pH 7·4 with TEA-OH (Cardenas *et al.* 1995). The internal solution used in the present study differed from that used previously in that much of the chloride ion was replaced by aspartate ion. This substitution prolonged the duration of recordings and reduced Ca^{2+} current rundown. However, the substitution produced an ~+10 mV shift in the threshold for activation of K^+ and Ca^{2+} currents which we routinely recorded. Thus, I_A was tested for by using a test potential of −50 mV rather than the −60 mV used previously and T-type Ca^{2+} currents were tested for by using a test potential of −30 mV rather than the −40 mV used previously (Cardenas *et al.* 1995).

For RT-PCR analysis a single DRG neuron was aspirated into a glass microelectrode. After aspiration, the electrode was broken and the contents (about 5 μl) ejected into a tube containing 5 μl of water, 1 μl of oligo(dT) (0·5 μg μl^{-1}) primer and 0·5 μl RNAsin (40 U ml^{-1}). Single-strand cDNA was synthesized from the cellular mRNA by adding 11 μl of RT Mix (4 μl water, 2 μl of 10X PCR buffer: 200 mM Tris-HCl (pH 8·4) and 500 mM KCl, 2 μl of 25 mM $MgCl_2$, 2 μl of 0·1 M dithiothreitol, 1 μl of mixed 10 mM deoxynucleotide triphosphates (dNTPs) and 1 μl of Super Script II RT (200 U μl^{-1}). The mixture was incubated for 50 min at 42 °C. The reaction was terminated by heating the mixture to 70 °C for 15 min and then submerging the container in an ice bath. The RNA strand in the RNA–DNA hybrid was then removed by adding 1 μl RNase H (2 U μl^{-1}) and incubating for 20 min at 37 °C. All reagents except for RNAsin (Promega) were obtained from Gibco-BRL.

The cDNA from the reverse transcription of RNA was further subjected to PCR. PCR amplification was carried out in a thermal cycler (MJ Research, Inc., Watertown, MA, USA) with thin-walled plastic tubes. The amplification program included 55 cycles: 94 °C for 1 min, 56 °C for 1 min and 72 °C for 1·5 min. The reaction mixture (30 μl) was composed of 1·5 μl of a 20 μM solution of each primer, 3 μl of cDNA template solution and 0·3 μl of Taq DNA polymerase (5 U μl^{-1}, Promega) to 23·7 μl of PCR MIX: 3 μl of 10X PCR buffer (100 mM Tris-HCl (pH 9·0), 500 mM KCl, 1% Triton X-100), 3 μl 25 mM $MgCl_2$, 1·5 μl 10 mM dNTPs and 16·2 μl water. The PCR primers used to amplify the $5\text{-}HT_{1D}$ nucleotide sequence fragments were: 5′-ACTCAGAATCTCCCTCG-TGGTGG-3′ and 5′-GTAGAGGGAGGGTGGGTTCAGGAT-3′ (598 bp product). To amplify $5\text{-}HT_7$ fragments, the primers were: 5′-GGTGGAAGAGTGTGCGAACCTTTC-3′ and 5′-CGGGCCT-CTCAGCAAGTTTCAG-3′ (383 bp product). To amplify $5\text{-}HT_{2C}$ fragments, the primers were: 5′-GCCGTCAAACTCTGATGTTAC-TTC-3′ and 5′-ACGTTCATTGGTATGCCGATAA-3′ (545 bp product).

After PCR, the products were separated by electrophoresis in 1·5% agarose gel stained with ethidium bromide. As a control for genomic contamination, samples were prepared as described above, except that the reverse transcriptase was omitted. These experiments consistently yielded negative results. As a control for contamination of primers and other solutions, PCR was also performed without cDNA for each experiment for each pair of primers.

Statistical analyses were performed using non-parametric tests; the Wilcoxon signed-rank test designed for paired samples or the Kruskal–Wallis one-way analysis of variance, designed for independent samples (Systat, SPSS Inc.). Probabilities of 0·05 or less were considered significant. Data are expressed as the means ± S.E.M. All statistical analysis regarding changes in the amplitude of I_H were performed on raw current data.

Holding the DRG cells at −40 or −50 mV minimized 5-HT-induced shifts in holding current which occurred at more negative holding potentials. This procedure facilitated the study of the effects of 5-HT on I_H activated by ~1–3 s long hyperpolarizing voltage commands. However, there appeared to be additional active current(s) which contributed to the fast current at holding potentials of −40 and −50 mV, which were reduced at more negative holding potentials (see Fig. 6*B* and *C*). Thus, no conclusions were drawn from fast currents in experiments where holding potentials of −40 or −50 mV were used. In addition, there appeared to be current(s) activated by repolarization to −40 or −50 mV, which contaminated the tail currents (see Fig. 6*B* and *C*). However, no conclusions were drawn from tail currents in this study.

RESULTS

The 5-HT-induced increase in hyperpolarization-activated current

Hyperpolarization of most medium- and large-diameter rat DRG cell bodies elicited an initial instantaneous and/or rapidly activating inward current (fast current) and a subsequent slowly activating inward current (slow current) (Fig. 2*A*). The effect of 5-HT (10 μM) was tested on the slow current amplitude in 43 medium-diameter (31·3–38 μm) DRG cells where the slow current was evoked by 787 ms test hyperpolarizations to −80 or −90 mV from a holding potential of −40 or −50 mV (Fig. 2*A*). In 39 of the 43 cells tested, 5-HT produced an increase in the slow current ranging from 5% to 40%. In three of the above-mentioned DRG cells, 100 nM 5-HT increased I_H by 10 ± 7 pA compared with an increase of 32 ± 10 pA produced by 1 μM 5-HT in the same cells, suggesting that the effect of 5-HT was concentration dependent. A 10 μM concentration of 5-HT appeared to be saturating, based on the observation that 50 μM 5-HT did not produce any further increase in three cells. The effects of 5-HT on the slow current were occluded by blocking I_H with Cs^{2+}, suggesting that the increase in the slow current was a result of increased conductance via I_H channels (Mayer & Westbrook, 1983; Scroggs *et al.* 1994). In five medium-diameter DRG cells where a control application of 10 μM 5-HT significantly increased the slow current by 45 ± 9 pA ($P < 0·05$, Wilcoxon signed-rank test), a subsequent challenge with 5-HT had no detectable effect on the current remaining in the presence of 1 mM Cs^+ (Fig. 2*B*).

The magnitude of the increase in I_H produced by 5-HT was dependent on the test potential used to evoke I_H. In six medium-diameter DRG cells studied, the largest increases in I_H produced by 5-HT (measured 787 ms after initiation of the voltage command) were observed at test potentials of −70 mV (68 ± 16 pA), −80 mV (87 ± 16 pA) and −90 mV (75 ± 15 pA) and represented increases over control current of 52 ± 16%, 27 ± 5% and 13 ± 3%, respectively (Fig. 2*C*). Thus, test potentials of −70, −80 and −90 mV appear most useful for studying the effects of 5-HT in DRG cells because the noise level is lowest relative to the increase

in current produced by 5-HT. To avoid excessively long hyperpolarizations, which tended to degrade the seal between the recording electrode and the cell membrane, the effect of 5-HT on I_H amplitude was usually assessed at a time point 787 ms after initiation of the voltage commands, before the current had fully activated. However, in these cases I_H was activated by test potentials to −80 or −90 mV and measurement of the current at later time points had little effect on the relative magnitude of the 5-HT effect (see Fig. 5*A*).

Characterization of DRG subpopulations exhibiting the 5-HT-induced increase in I_H

In order to assess the possibility that 5-HT was targeting I_H in some subpopulations of DRG cells but not others, the effect of 5-HT on hyperpolarization-activated currents was observed in DRG cells which were classified as type 1, 2, 3 or 4 based on the expression of I_H, I_A, capsaicin sensitivity and T-type Ca^{2+} currents as described in Methods (see Fig. 1*A* and *B*) (Cardenas *et al.* 1995). In 13 of 14 DRG cells classified as type 4, 5-HT (10 μM) increased I_H evoked by

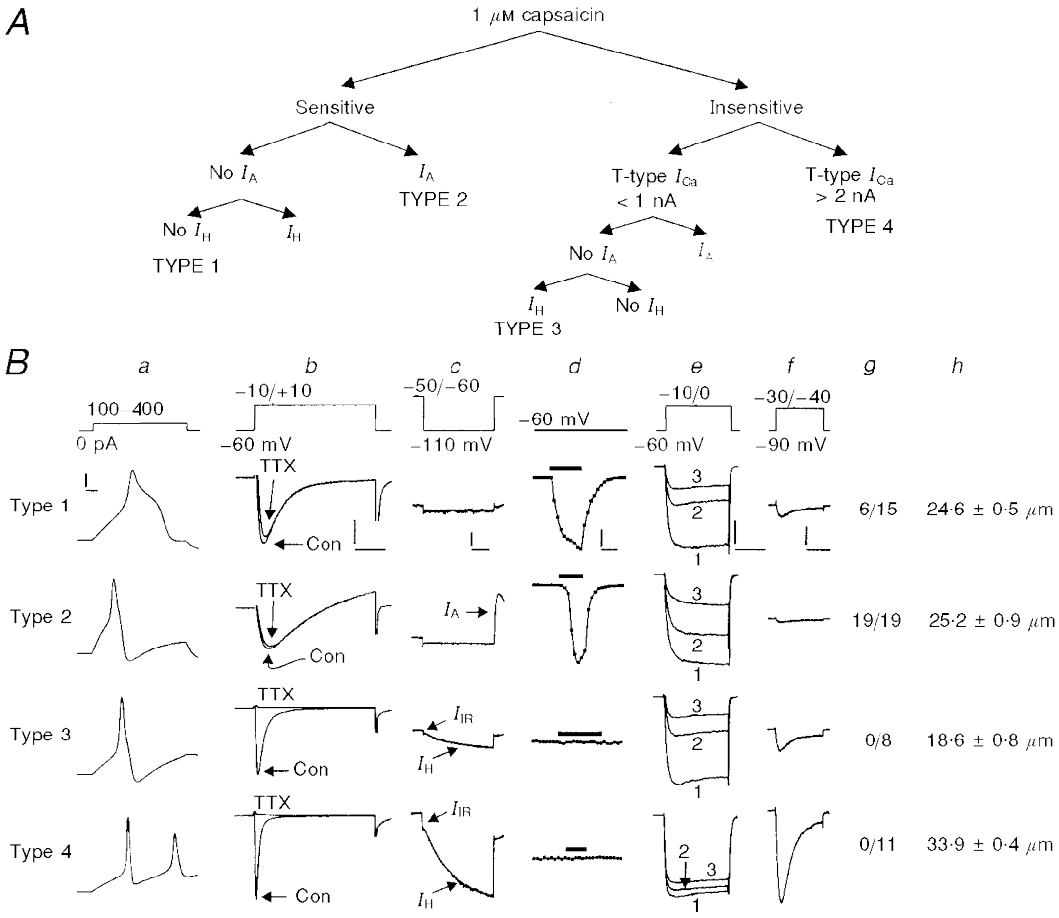

Figure 1. Type 1–4 DRG cells

A, dichotomous key for grouping DRG cells (modified from Cardenas *et al.* 1995). *B*, characteristics of type 1–4 DRG cells. The current or voltage clamp protocol is illustrated at the top of each column (*a–f*), except for that used to detect I_{IR} (voltage commands ranging from −70 mV to −120 mV, in 10 mV increments, from a holding potential of −60 mV). *a*, action potentials. *b*, Na^+ currents in the absence and presence of 1 μM TTX. Con, control. *c*, expression of I_H, I_A and I_{IR}. I_{IR} was apparent in about 50% of type 3 cells and nearly all type 4 DRG cells. *d*, effects of (1 μM) capsaicin on holding current. The bars represent the time course of capsaicin application. *e*, L- and N-type Ca^{2+} channel currents recorded under control conditions (1), after L-channel blockade with 2 μM nimodipine (2), and after the subsequent blockade of N-channels with nimodipine + 1 μM ω-conotoxin GVIA (3). *f*, T-type Ca^{2+} channel currents. *g*, number of DRG cells out of the total tested which expressed the lactoseries surface antigen Galβ1-4 GlcNAc-R, characteristic of a subpopulation of afferents terminating in lamina I and II of the spinal cord. *h*, average cell diameter. $n = 34$, 19, 21 and 23 for types 1–4, respectively. The vertical calibration bars are: 20 mV (*a*), 1 nA for types 1–3 and 4 nA for type 4 (*b*), 400 pA for type 1 and 800 pA for types 2–4 (*c*), 200 pA for type 1, 1·2 nA for type 2 and 1 nA for types 3–4 (*d*), 1 nA for types 1–3 and 2 nA for type 4 (*e*), and 400 pA for types 1–3 and 1 nA for type 4 (*f*). The horizontal calibration bars are: 3 ms (*a*), 6 ms (*b*), 200 ms (*c*), 12·5 ms (*d*), 20 ms (*e*) and 80 ms (*f*). The data are from Cardenas *et al.* 1995 (*a*, *c*, *d*, *e*, *f* and *h*); Cardenas *et al.* 1997*b* (*b*); and Del Mar & Scroggs, 1996 (*g*).

hyperpolarizations to −90 mV from a holding potential of −50 mV. The average increase for all 14 cells (39 ± 5 pA) was significant ($P < 0{\cdot}05$, Wilcoxon signed-rank test) and represented a 12 ± 2% increase over control I_H amplitude (Fig. 3*D*). 5-HT (10 μM) also increased I_H in nine of 14 large-diameter (45–52·5 μm) DRG cells tested (Fig. 2*E*). In the nine large-diameter DRG cells which were sensitive to 5-HT, I_H evoked by a 787 ms hyperpolarization to −110 mV from a holding potential of −60 mV was increased by an average of 257 ± 91 pA, which represented a 10 ± 1% increase over control I_H amplitude (Fig. 2*E*).

In contrast, 10 μM 5-HT did not significantly affect hyperpolarization-activated currents in the smaller-diameter type 1 or type 2 DRG cells (average diameter, 22·4 ± 0·7 and 24·1 ± 0·6 μm; $n = 9$ and 11, respectively). These categories of DRG cells characteristically exhibit little (type 2) or no (type 1) I_H under control conditions (Fig. 1*Bc*). Similarly, 10 μM 5-HT did not increase I_H in type 3 DRG cells, which are also small in diameter (average diameter, 19·2 ± 0·3 μm; $n = 8$), but characteristically express I_H under control conditions (Fig. 1*Bc*). Finally, 10 μM 5-HT did not significantly affect hyperpolarization-activated currents in nine additional small-diameter DRG cells (average diameter, 20·8 ± 1·3 μm), which did not fit into the type 1, 2, 3 or 4 categories.

Characterization of the receptor mediating the 5-HT-induced increase in I_H

The 5-HT receptor subtype mediating the effects of 5-HT on I_H in medium-diameter DRG cells was explored using selective 5-HT receptor ligands. As illustrated in Fig. 3*Aa–c*, the increase in I_H produced by 5-HT in medium-diameter DRG cells was mimicked by the 5-HT receptor agonist

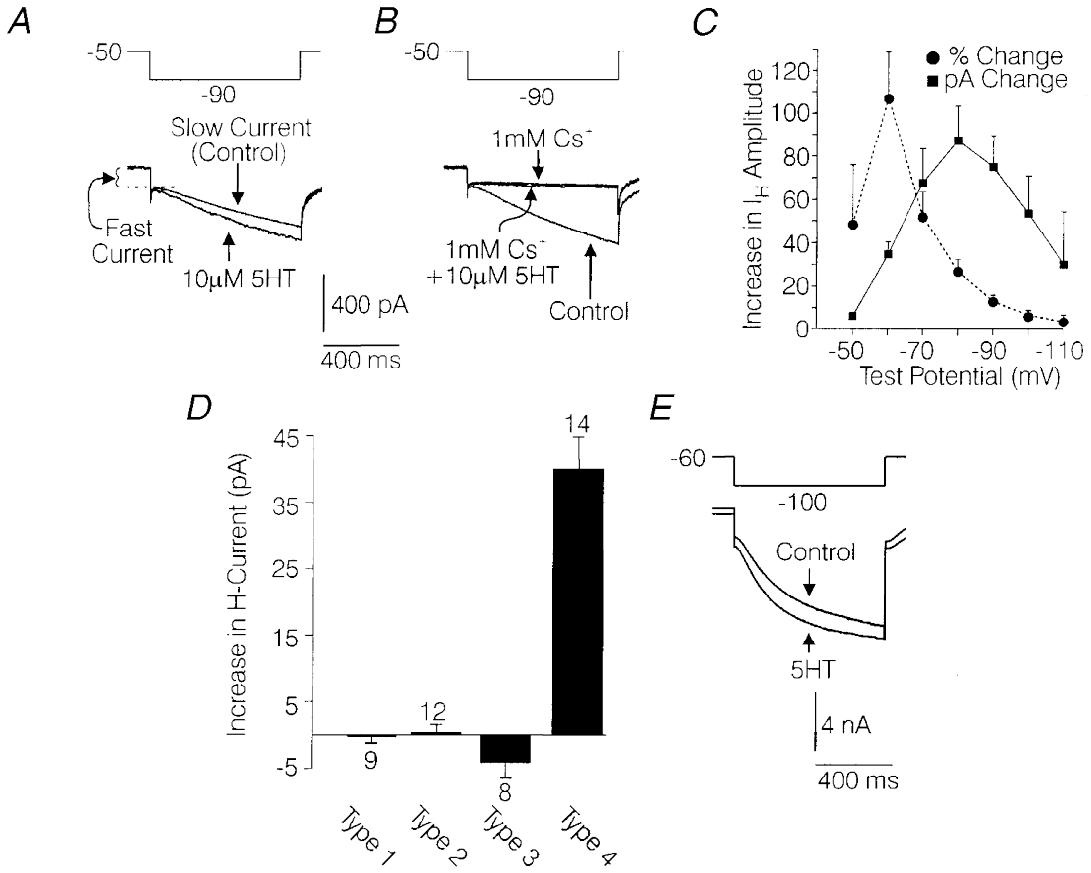

Figure 2. Enhancement of I_H by 5-HT, selectively in distinct subpopulations of DRG cells

A, effect of 5-HT on the slowly activating inward current (slow current) evoked by a 787 ms hyperpolarization to −90 mV from a holding potential of −50 mV in a medium-diameter DRG cell. *B*, effects of Cs^+ on the slow current and effects of 5-HT on the current remaining in the presence of Cs^+ in the same cell as *A*. *C*, plot of the 5-HT (10 μM)-induced increase in I_H amplitude *versus* voltage. I_H amplitude was measured 787 ms after initiation of the voltage commands. ●, percentage change; ■, actual change (in pA). For each point, $n = 6$ medium-diameter cells. Error bars show the S.E.M. *D*, bar-graph illustrating the average effect of 10 μM 5-HT on inward current present at the end of a 787 ms hyperpolarization to −90 mV from a holding potential of −50 mV in DRG cells characterized as type 1, 2, 3 and 4 as described in Methods. Error bars show the S.E.M. Numbers above or below the bars, indicate the number of cells (n). *E*, effect of 10 μM 5-HT on I_H in a large-diameter DRG cell. External and pipette solutions are given in Methods.

5-CT, but not by 8-OH-DPAT. The percentage change in I_H produced by the 5-HT receptor agonists in five medium-diameter cells, each tested with all three agonists, is summarized in the bar-graph shown in Fig. 3*D*. Both 5-CT and 5-HT significantly increased I_H, by 70 ± 14 and 60 ± 11 pA, respectively ($P < 0{\cdot}05$, Wilcoxon signed-rank test). 8-OH-DPAT did not have a significant effect on I_H (average change, -18 ± 8 pA). The effect of 5-HT and 5-CT on I_H had a similar time course, i.e. a gradual increase in amplitude which peaked within approximately 1 min following the onset of drug administration and which reversed within 2 min of the onset of drug washout (Fig. 3*Aaa–cc*).

In addition to being mimicked by 5-CT, the effect of 5-HT on I_H was potently blocked by spiperone. As illustrated in Fig. 3*Ba*, *Bb* and *E*, I_H was not changed significantly by 1 μM 5-HT when 5-HT was added in the presence of 1 μM spiperone (average change, -3 ± 10 pA). However, after 3 min of wash with Tyrode solution, 1 μM 5-HT significantly increased I_H by 39 ± 7 pA ($P < 0{\cdot}05$, Wilcoxon signed-rank test), indicating that the cells included were sensitive to 5-HT. The order of addition of drugs was designed to ensure that any attenuation of the effects of 5-HT on I_H due to repeated application was not interpreted as antagonism. Spiperone plus vehicle (0·1 % DMSO, final concentration) did not have any detectable effect on I_H. Also, in two medium-diameter DRG cells tested, 5-HT was observed to produce a typical increase in I_H in the presence of DMSO (0·1 %), indicating that DMSO did not antagonize the effects of 5-HT.

An additional observation was that 1 μM cyanopindolol failed to antagonize the effects of 1 μM 5-HT on I_H amplitude. The experiments with cyanopindolol were carried out in the same manner as described for spiperone, except that the DRG cells were held at −40 mV instead of −50 mV and were given voltage commands to −80 mV instead of −90 mV (Fig. 3*Ca* and *b*). In the presence of cyanopindolol 5-HT increased I_H by 69 ± 13 pA, while after a wash period of 3 min in Tyrode solution, a second application of 5-HT increased I_H by 53 ± 11 pA (Fig. 3*Ca*, *Cb* and *F*. Cyanopindolol alone did not have a significant effect on I_H amplitude (Fig. 3*F*). Note that on average the initial challenge with 5-HT in the presence of cyanopindolol produced a larger increase in I_H than that produced by a second challenge with 5-HT alone. This pattern is probably attributable to attenuation of the 5-HT-induced increase in I_H, which usually occurred with repeated applications of 5-HT. As elaborated in the Discussion, the above battery of pharmacological tests point most strongly to the 5-HT_7 receptor subtype as mediating the effects of 5-HT on I_H. However, 5-HT_{1D} and 5-HT_{2C} receptors cannot be conclusively ruled out based on this data alone.

Detection of 5-HT_{1D}, 5-HT_7 and 5-HT_{2C} receptor mRNA in medium-diameter DRG cells using RT-PCR analysis

The expression of the genes for rat 5-HT_{1D}, 5-HT_7 and 5-HT_{2C} receptors was tested for in individual medium-diameter DRG cells (33–38 μm in diameter, $n = 10$) by means of single-cell RT-PCR (see Methods). Individual medium-diameter DRG neurons were isolated and their mRNA was reverse transcribed into cDNA. Then the cDNA was subjected to PCR with the specific primers for rat 5-HT_{1D}, 5-HT_7 and 5-HT_{2C} receptors. The amplicons were separated by electrophoresis and their size estimated by comparison with size markers run alongside in each gel. Figure 4 illustrates the results from a medium-diameter DRG cell which was positive for 5-HT_7 and 5-HT_{1D} receptor mRNA. 5-HT_7 receptor mRNA was detected in nine out of ten DRG cells tested, while 5-HT_{1D} receptor mRNA was detected in four out of six cells tested. 5-HT_{2C} receptor mRNA was not detected in any of eight individual medium-diameter DRG cells tested, even though it was readily demonstrated in whole DRG. The above RT-PCR data support the idea that 5-HT_7 or 5-HT_{1D} receptors mediate the effects of 5-HT on I_H and argue against the involvement of 5-HT_{2C} receptors.

5-HT receptor coupling to I_H channels

As illustrated in Fig. 5*A* and *B*, 5-HT produced a shift in the conductance–voltage relationship for I_H. The activation of I_H was studied by applying 2·35 s voltage commands to −50 mV through −120 mV, in 10 mV increments, from a holding potential of −40 mV. The peak conductance at each voltage was modelled with the Boltzmann equation:

$$g = g_{max}/(1 + \exp((V_m - V_{½})/k)),$$

where g is the conductance ($I/V_m - V_r$), V_m is the membrane potential, $V_{½}$ is the membrane potential where I_H is 50 % activated and k is the slope constant. The reversal potential (V_r) for I_H used to calculate conductance was −23 mV as determined in this study (see Fig. 8). The best fit values for $V_{½}$ and k were determined by fitting the data regarding conductance *versus* voltage with the above equation using a simplex least-squares iteration program (Systat, SPSS Inc.). In six medium-diameter DRG cells studied, 5-HT (10 μM) significantly shifted $V_{½}$ by $+6 \pm 0{\cdot}3$ mV, from an average control value of $-73 \pm 0{\cdot}6$ mV, to $-67 \pm 0{\cdot}9$ mV (Wilcoxon signed-rank test, $P < 0{\cdot}05$) (Fig. 5*A* and *B*). Peak conductance (g_{max}) and the slope constant (k) were not significantly affected by 5-HT, averaging $13{\cdot}9 \pm 2{\cdot}8$ nS and $7 \pm 0{\cdot}3$ under control conditions and $14 \pm 2{\cdot}8$ nS and $6{\cdot}9 \pm 0{\cdot}3$ in the presence of 5-HT, respectively. The estimates of ∼−73 mV for $V_{½}$ and ∼7 for the slope constant k under control conditions are similar to values obtained for I_H in neurons by other investigators using I_H activated by hyperpolarizing voltage commands, or using tail currents in the presence of similar intracellular and extracellular concentrations of K^+ and Na^+ (Hestrin, 1987; Travagali & Gillis, 1994; Ingram *et al.* 1996; Raes *et al.* 1997; for review, see Pape, 1996).

The 2·35 s time course of the hyperpolarizing voltage command was chosen because I_H was almost completely activated during this time for all voltages tested, while complete activation took much longer. Data collected at

maximal activation was likely to be marred by desensitization of the 5-HT effect and current rundown, due to the longer overall time needed to collect the data for each treatment. In order to estimate the error induced by collecting the data when the current was not fully activated, an estimate of I_H amplitude at full activation was extrapolated by fitting the control currents in the cell depicted in Fig. 5*A* and *B* with the double exponential expression:

$$I = I_f(1 - \exp(-x/\tau_f)) + I_s(1 - \exp(-x/\tau_s)).$$

In this expression I_f and I_s represent the amplitudes of rapidly and slowly activating components of I_H, which activate with the time constants τ_f and τ_s, respectively, and x represents the time after initiation of the voltage command (Fig. 5*C*). Best fit values for I_f, I_s, τ_f and τ_s were estimated using the simplex least-squares iteration program. Curves generated by the above equation using the best fit values were extrapolated out to a time point 10 s after the initiation of the voltage commands, where they had all reached maximum amplitude (Fig. 5*C*). When the conductance–voltage relationship was recalculated using the extrapolated current amplitudes, $V_{½}$ was shifted by +2·7 mV. This analysis suggests that only a small error was introduced by measuring the current amplitude at the 2·35 s time point.

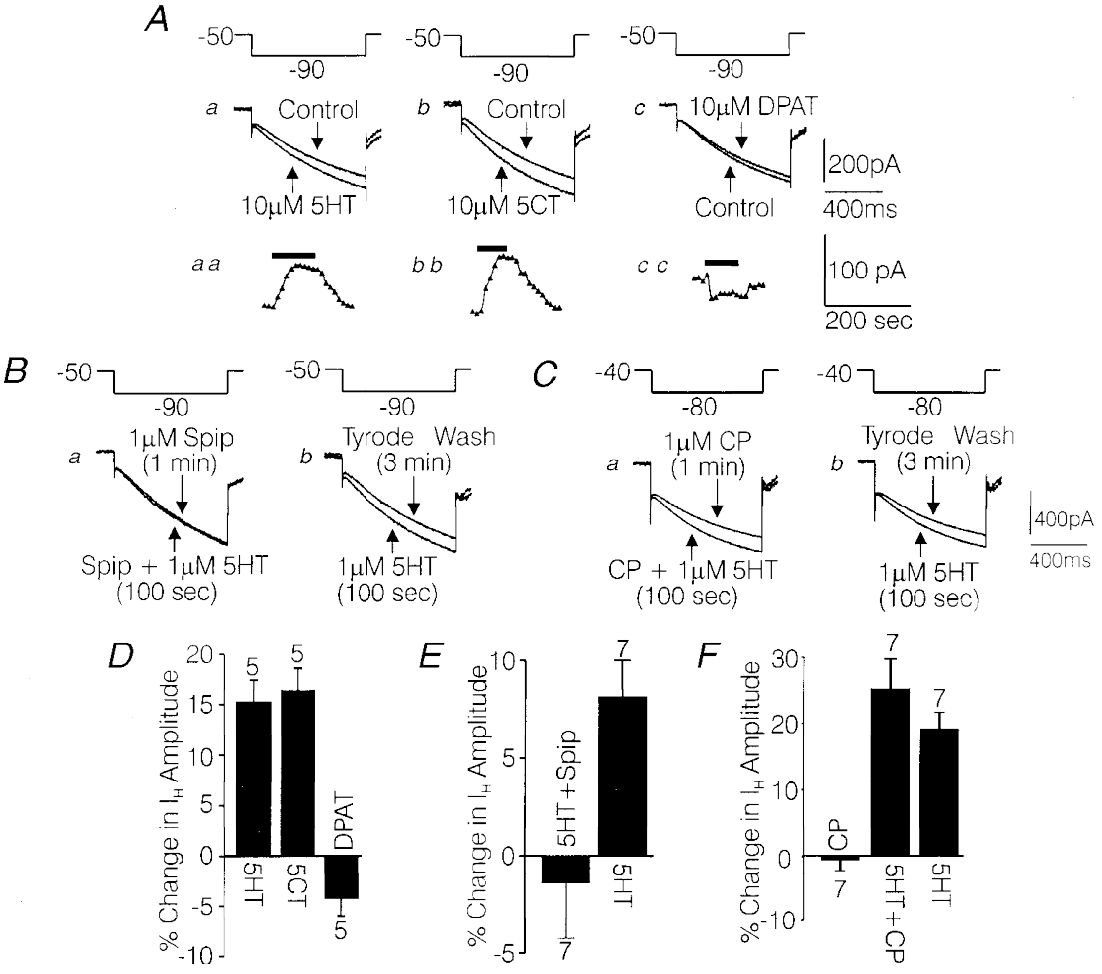

Figure 3. Pharmacological characterization of the 5-HT receptor mediating the effects of 5-HT on I_H

A, individual current traces recorded from a medium-diameter DRG cell under control conditions and during the peak effect of 10 μM 5-HT (*a*), 10 μM 5-CT (*b*) and 10 μM 8-OH-DPAT (*c*). The insets *aa*, *bb* and *cc* are graphs of change in I_H over time for each agonist. Arrows show measurements taken at 10 s intervals. Changes in fast current were subtracted. *B*, effect of 1 μM 5-HT on I_H when tested in the presence of 1 μM spiperone (Spip) (*a*) and after spiperone was washed off for 3 min (*b*). *C*, effect of 1 μM 5-HT on I_H when tested in the presence of 1 μM (±)cyanopindolol (CP) (*a*) and after cyanopindolol was washed off for 3 min (*b*). *D*, bar-graph summarizing the effects of the 3 agonists tested in *A*, in 5 cells where all 3 agonists were tested on each cell. *E*, bar-graph summarizing the antagonism of 1 μM 5-HT by spiperone in 7 medium-diameter DRG cells. *F*, bar-graph summarizing the effects on I_H of 1 μM cyanopindolol, 1 μM cyanopindolol + 1 μM 5-HT and 1 μM 5-HT alone after a 3 min washout in 7 medium-diameter DRG cells. The solutions were the same as those used to record I_H in Fig. 2.

The 5-HT-induced shift in the conduction–voltage relationship for I_H resembles changes in I_H produced via activation of cAMP-dependent signalling pathways. (Ludwig *et al.* 1998). This idea was explored using the adenylyl cyclase activator forskolin. Forskolin (10 μM) significantly increased I_H amplitude by 116 ± 24 pA (Wilcoxon signed-rank test, $P < 0{\cdot}05$, $n = 6$) (Fig. 5*D* and *F*) and was observed to produce a positive shift in the conductance–voltage relationship for I_H in two cells (data not shown). Also, forskolin significantly occluded the effects of 5-HT on I_H. The amplitude of I_H was not significantly increased by 5-HT (10 μM) when 5-HT was added in the presence of forskolin (average change, 8 ± 15 pA) (Fig. 5*D* and *F*). However, after washout of the forskolin and 5-HT for 6–7 min, reapplication of 5-HT significantly increased I_H amplitude by 75 ± 9 pA ($P < 0{\cdot}05$, Wilcoxon signed-rank test), demonstrating that the cells were still sensitive to 5-HT (Fig. 5*E* and *F*). An inactive form of forskolin (1,9-dideoxy forskolin, 10 μM) did not significantly affect I_H amplitude (Fig. 5*F*). The increase in I_H produced by forskolin and the occlusion of the effects of 5-HT by forskolin is consistent with the idea that an increase in cAMP mediates the effects of 5-HT on I_H.

Voltage dependence of the effects of 5-HT on steady-state inward current, fast current and evoked I_H

The effects of 5-HT on steady-state inward current and fast current exhibited a pronounced voltage dependence. As illustrated in Fig. 6, application of 5-HT to medium-diameter DRG cells held at −50 mV produced a negligible change in steady-state inward current (average, 3 ± 3 pA, $n = 3$) and fast current (3 ± 4 pA, $n = 3$) evoked by a voltage command to −90 mV (Fig. 6*A* and *B*). However, when the same DRG cells were held at −70 mV, reapplication of 5-HT produced a large increase in steady-state inward current and fast current amplitude, which averaged 93 ± 24 and 38 ± 12 pA, respectively (Fig. 6*A* and *C*). The effects of 5-HT on I_H evoked during the course of 787 ms hyperpolarizing voltage commands also displayed voltage dependence. When the same DRG cells mentioned above were held at −70 mV, 5-HT produced a decrease of 8 ± 5% in I_H activated during the hyperpolarizing voltage command, compared with the 18 ± 4% increase in I_H observed when the same three cells were held at −50 mV (Fig. 6*B* and *C*). The voltage dependence of the 5-HT effects on steady-state inward current and fast current were probably the result of differences in the number of I_H channels which were shifted into a tonically open state by 5-HT at different holding potentials. In turn, increasing the number of tonically activated I_H channels probably reduces the pool of channels available for activation by a hyperpolarizing voltage command.

Identity of the ion current mediating the 5-HT-induced increase in steady-state inward current and fast current

Although the observed changes in steady-state inward current and fast current produced by 5-HT at a holding potential of −70 mV can be adequately explained by changes in I_H, it seemed possible that other ion currents

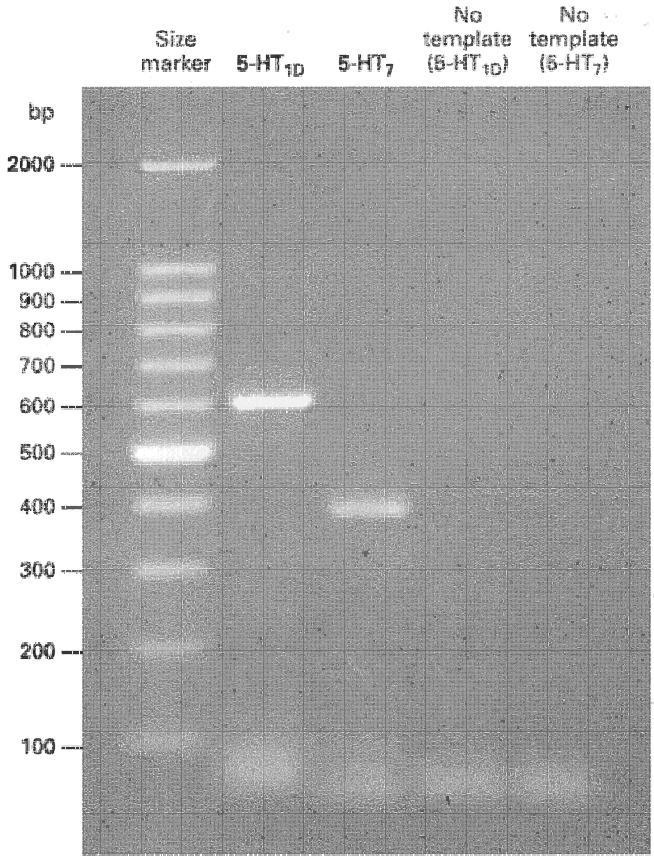

Figure 4. Photograph of an ethidium bromide-stained agarose gel demonstrating the expression of mRNA for 5-HT_{1D} and 5-HT_7 receptors in an individual medium-diameter DRG cell

Lane 1 (far left), size markers consisting of nucleotide chains of different lengths. Lanes 2 and 3, separation of 5-HT_{1D} and 5-HT_7 serotonin receptor amplicons, respectively. The predicted size for the 5-HT_{1D} amplicon is 598 nucleotides and the predicted size for the 5-HT_7 amplicon is 383 nucleotides. Lanes 4 and 5, negative PCR controls, where cDNA templates were omitted from the PCR.

potentially modulated by 5-HT (such as the prominent inward rectifier expressed by most medium-diameter DRG cells, see Fig. 7*B* and *D*) might modify or contribute to these 5-HT effects. This possibility was explored by studying the interaction of Cs^+ and Ba^{2+} with the effects of 5-HT on steady-state inward current and fast current in medium-diameter DRG cells held at −60 mV.

Steady-state inward current. In seven medium-diameter DRG cells held at −60 mV, 5-HT increased steady-state inward current by 95 ± 22 pA. As illustrated in Fig. 7*A*, the increase in steady-state inward current produced by 5-HT at a holding potential of −60 mV was repeatable, although typically the response diminished in amplitude with successive trials. In five medium-diameter DRG cells tested in the presence of 1 mM Cs^+, 10 μM 5-HT increased steady-state inward current by only 18 ± 3 pA, compared with an increase of 88 ± 40 pA produced by reapplication of 5-HT after washout of Cs^+ ($P < 0{\cdot}05$, Wilcoxon signed-rank test) (Fig. 7*A*). The comparison of the effects of 5-HT

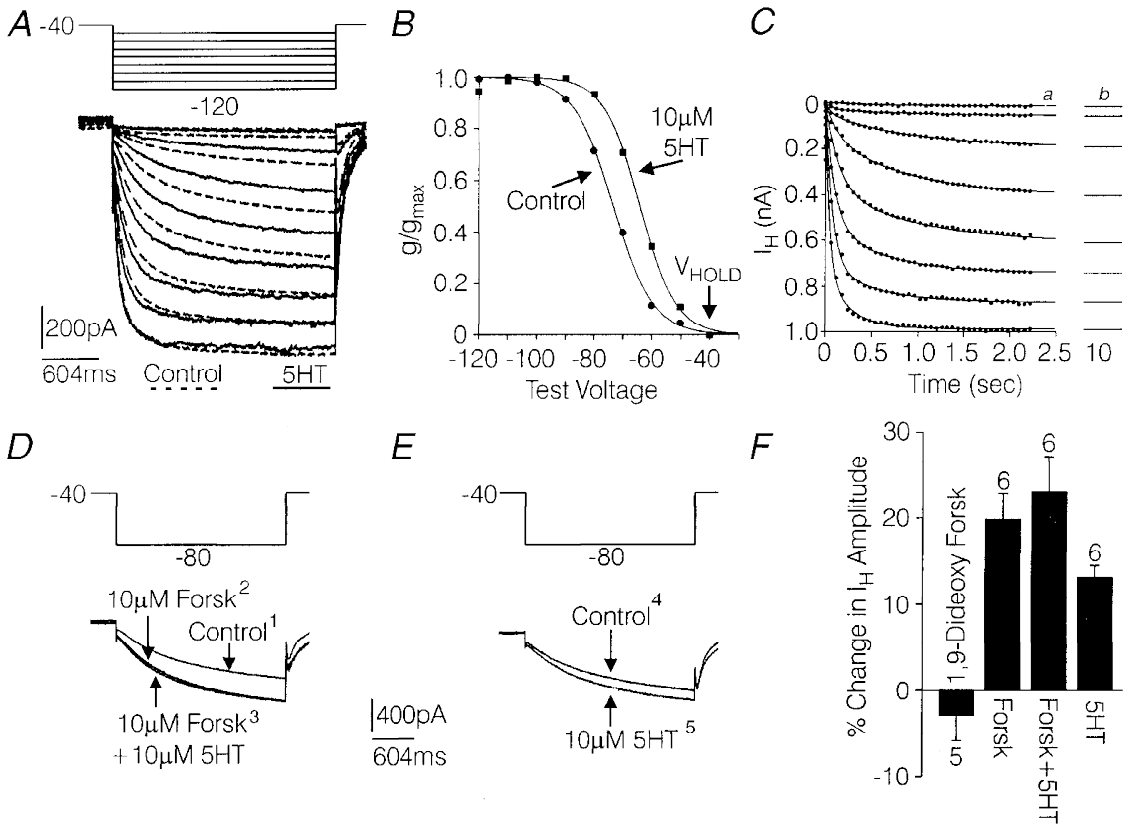

Figure 5. Coupling of 5-HT receptors with I_H in medium-diameter DRG cells

A, I_H evoked by a series of voltage commands ranging from −50 mV to −120 mV, in 10 mV increments, from a holding potential of −40 mV, under control conditions (black lines) and in the presence of 10 μM 5-HT (dashed lines). *B*, conductance–voltage relationship for the I_H shown in *A*. The amplitude of I_H at each voltage was measured 2·35 s after the initiation of the voltage command and converted to conductance as described in the text. Peak conductance was 7·82 nS under control conditions and 7·87 nS in the presence of 5-HT. Best fit values for $V_{½}$ and k were obtained by fitting the normalized conductance data with a Boltzmann function as described in the text. For I_H recorded under control conditions and in the presence of 5-HT, respectively, the best fit values were −73·3 and −64·1 mV for $V_{½}$ and were 7·0 and 6·3 for k. Curves fitted to the data in *B* were generated with the Boltzmann equation using the best fit values. *C*, analysis of completeness of activation of I_H at all voltages tested in *A* at the time point of 2·35 s. The filled circles represent measurements of I_H amplitude from *A* at 60 ms intervals. The measurements of I_H at each voltage tested were fitted with a double exponential expression and best fit values for I_f, I_s, τ_f and τ_s were estimated as described in the text. Curves generated with the double exponential equation using the best fit values (*a*) were extrapolated out to 10 s (*b*) where they had reached maximum amplitude. *D*, effects of 10 μM forskolin on I_H in a medium-diameter DRG cell (1 and 2) and effects of 10 μM 5-HT on I_H in the continued presence of forskolin (3). *E*, effects of subsequent re-application of 5-HT after the effects of the previous treatments had been washed out with control Tyrode solution (4 and 5). The numbers represent the order in which the currents were recorded. *F*, summary of the above experiment in 6 medium-diameter DRG cells and the effects of inactive 1,9-dideoxy forskolin in 5 of the 6 cells. Error bars show the S.E.M. Solutions were the same as those used to record I_H in Fig. 2.

in the presence of Cs^+ with the effects of 5-HT after washout of Cs^+ was designed to control for the attenuation of the 5-HT response with repeated trials. In contrast, the effects of 5-HT on steady-state inward current were not significantly altered by Ba^{2+} (Fig. 8*A*). In five medium-diameter cells tested in the presence of 100 μM Ba^{2+}, 10 μM 5-HT increased steady-state inward current by 114 ± 24 pA, similar to the 95 ± 22 pA increase in steady-state inward current produced by 5-HT in the absence of Ba^{2+} (as reported above). The combined data regarding Ba^{2+} and Cs^+ indicate that the majority of the 5-HT-induced increase in steady-state inward current was due to an increase in tonically activated I_H (which is blocked by Cs^+ but not Ba^{2+}), with negligible modification resulting from the putative effects of 5-HT on the inward rectifier (which is blocked by both Ba^{2+} and Cs^+).

Fast current. In the same seven medium-diameter DRG cells, 10 μM 5-HT increased fast current evoked by test potentials to −120 mV by 181 ± 49 pA (Fig. 7*B*). In order to clarify the effects of 5-HT on fast current, the effects of Ba^{2+} and Cs^+ were first studied on fast currents evoked by voltage commands to −120 mV from a holding potential of −60 mV in the absence of 5-HT. Fast current was defined as the point of least current in each current trace, in order to minimize contamination of the measurements with current spent charging the whole-cell capacitance or I_H activated by the test hyperpolarization (see Figs 7*B* and *C* and 8*B*). Both 1 mM Cs^+ and 100 μM Ba^{2+} eliminated the inward rectification of the fast current *I–V* relationship (see Figs 7*D* and 8*D*). However, Cs^+ blocked 87 ± 2% ($n = 5$) of the fast current, which was significantly greater than the 58 ± 6% ($n = 6$) blockade produced by 100 μM Ba^{2+} ($P < 0{\cdot}05$ Kruskal–Wallis one-way analysis of variance). Together, this data suggests that approximately 87% of the fast current evoked by a test hyperpolarization to −120 mV can be accounted for by two components; a fraction with an inwardly rectifying *I–V* relationship, which is blocked by either 100 μM Ba^{2+} or 1 mM Cs^+, and a fraction with a linear *I–V* relationship, which is blocked by 1 mM Cs^+, but not by 100 μM Ba^{2+}. It appeared possible that either of these components could participate in the 5-HT-induced increase in fast current.

The potential effects of 5-HT on the linear *versus* the inwardly rectifying component were examined by studying the ability of Cs^+ or Ba^{2+} to occlude the effect of 5-HT on the fast current. As illustrated in Fig. 7*B–D*, Cs^+ almost completely occluded the effects of 5-HT on fast current. In the presence of Cs^+, the 5-HT-induced increase in fast current averaged only 1 ± 1 pA (Fig. 7*C*) compared with an increase of 48 ± 21 pA observed after Cs^+ was washed off the cells ($P < 0{\cdot}05$, Wilcoxon signed-rank test, $n = 5$). By contrast, the effect of 5-HT on fast current was not significantly affected by Ba^{2+} (Fig. 8*B*). In the presence of 100 μM Ba^{2+}, 10 μM 5-HT increased fast current by 178 ± 33 pA ($n = 5$) compared with an increase of 181 ± 49 pA ($n = 7$) produced by 5-HT in the absence of Ba^{2+} in a different group of cells. These data suggest that the 5-HT-induced increase in fast current was due to an increase in the linear component, which was blocked by Cs^+ but not Ba^{2+} (similar to I_H), rather than the inwardly rectifying component, which was potently blocked by Ba^{2+}.

To test further the idea that the 5-HT-induced increase in steady-state inward current and fast current represented

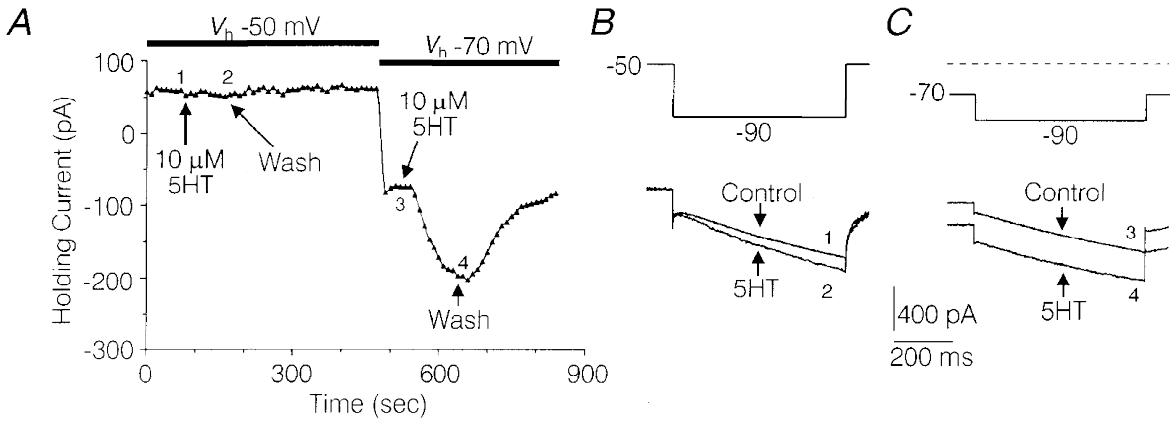

Figure 6. Interaction of holding potential with the effects of 5-HT on holding current, fast current and slow current

A, plot of holding current *versus* time illustrating the effect of 5-HT on holding current at a holding potential (V_h) of −50 mV *versus* a V_h of −70 mV. At each data collection point (arrows), at 10 s intervals, a 787 ms hyperpolarizing test command to −90 mV was initiated. *B* and *C*, current sweeps taken from the experiment depicted in *A*, illustrating the effects of 5-HT on fast and slow current under control conditions and during the peak effect of 5-HT at each holding potential. The numbers next to the traces designate where they were taken from in the experiment depicted in *A*. Solutions were the same as those used to record I_H in Fig. 2.

increased tonic I_H, the net reversal potential of the 5-HT-sensitive component of fast current (determined in the presence of 100 μM Ba^{2+}) was compared with the reversal potential for I_H (also determined in the presence of 100 μM Ba^{2+}). As illustrated in Fig. 8*B* and *D*, the reversal potential extrapolated from the *I–V* relationship of the fast currents under control conditions and during the peak effect of 5-HT averaged $-22{\cdot}5 \pm 1{\cdot}4$ mV ($n = 5$). This was similar to the reversal potential of $-22{\cdot}7 \pm 2{\cdot}4$ mV ($n = 5$) obtained in another group of medium-diameter DRG cells for the portion of fast current which was increased by changing the holding potential from −60 to −80 mV, in the presence of Ba^{2+} (Fig. 8*C* and *E*). In the presence of Ba^{2+} to block the inwardly rectifying conductance, the increase in fast current produced by the shift in holding potential predominantly reflects an increase in tonically open I_H channels (Mayer & Westbrook, 1983).

Effects of 5-HT on resting membrane potential, input resistance and anode-break excitation

In order to explore the possible physiological roles of the enhancement of I_H by 5-HT, the effects of 5-HT on resting membrane potential, input resistance and anode-break excitation were studied in five medium-diameter DRG cells. As illustrated in Fig. 9*A*, 5-HT (10 μM) produced a significant depolarization of the resting membrane potential. Under control conditions, the resting membrane potential in five medium-diameter neurons studied averaged $-53{\cdot}8 \pm 1{\cdot}6$ mV and was significantly depolarized to $-47{\cdot}6 \pm 2{\cdot}2$ mV in the presence of 5-HT ($P < 0{\cdot}05$, Wilcoxon signed-rank test) (Fig. 9*A*).

In the same five cells, the effects of 5-HT on input resistance and anode-break excitation were simultaneously monitored. For this experiment the amplitude of a 395 ms hyperpolarizing current pulse was adjusted in 10 pA increments

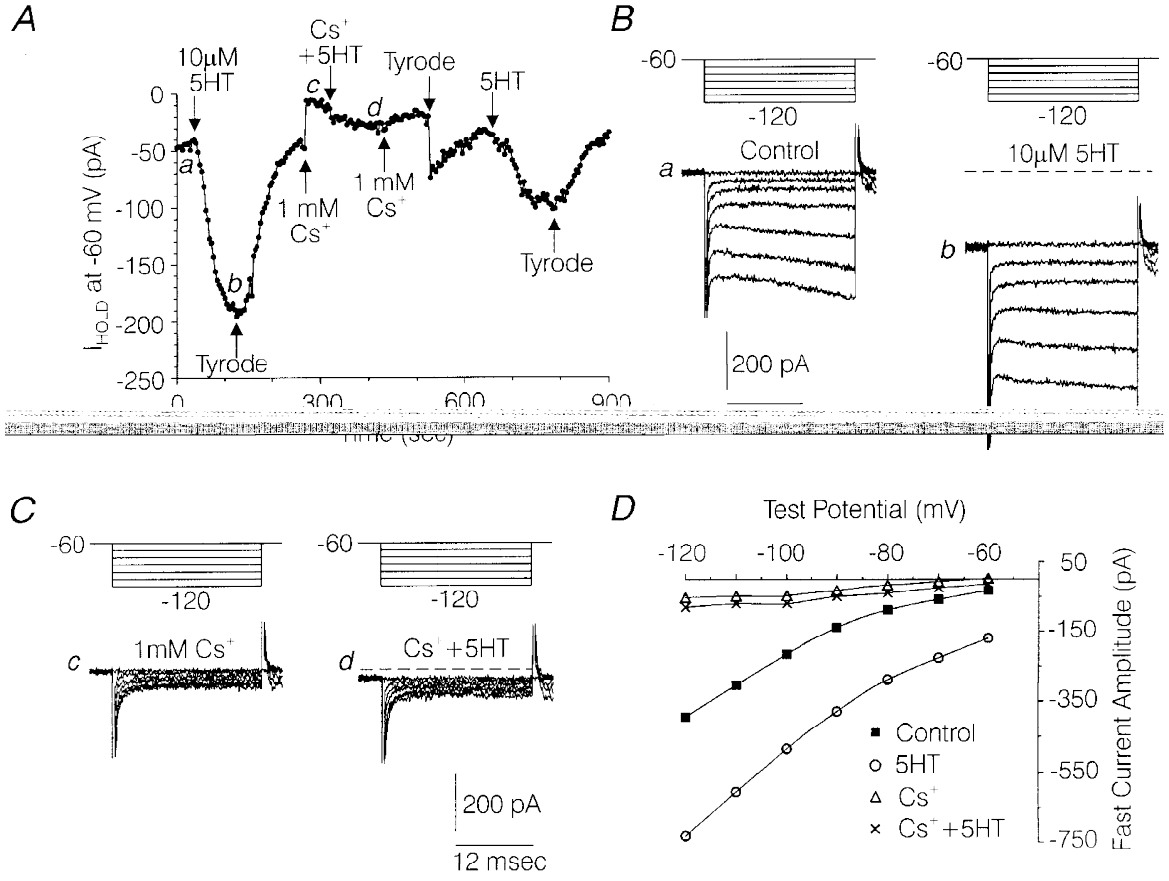

Figure 7. Blockade of the effects of 5-HT on holding current and fast current by Cs^+

A, plot of holding current (I_{hold}) at a holding potential of −60 mV *versus* time, illustrating the effects of 5-HT in the absence and presence of 1 mM Cs^+ and again after washout of Cs^+. *B*, families of current sweeps taken from the experiment depicted in *A*, under control conditions (*a*) and during the peak effect of 10 μM 5-HT (*b*). *C*, families of current traces from the above experiment in the presence of 1 mM Cs^+ (*c*) and 1 mM Cs^+ + 10 μM 5-HT (*d*). In *B* and *C*, each family of currents was generated by a series of 22 ms hyperpolarizations ranging from −70 to −120 mV from a V_h of −60 mV. *a*, *b*, *c* and *d* indicate the locations from which the traces were taken in *A*. *D*, plot of the fast current amplitude *versus* the command voltage for *a* (■) and *b* (○) in *B* and *c* (△) and *d* (×) in *C*. Fast current amplitude was measured at the point of least current in each trace. Solutions were the same as those used to record I_H in Fig. 2.

for each cell until the threshold for anode-break excitation was reached. The required current amplitude varied from −20 pA to −100 pA. Based on this current injection protocol, input resistance averaged 379 ± 46 MΩ under control conditions and 345 ± 31 MΩ during the peak depolarization produced by 5-HT (Fig. 9*Ba* and *b*). The effect of 5-HT on input resistance was not significant when the cells remained depolarized in the presence of 5-HT. However, when the membrane potential was clamped back to control levels by constant current injection in four of the above cells, a dramatic decrease in input resistance was unmasked in each case (Fig. 9*A* and *Bb*).

In the above-mentioned five medium-diameter DRG cells, the excitatory response to cessation of the hyperpolarizing current pulse (anode-break) was characterized by a long-duration depolarization which gave rise to action potentials. Previous studies have demonstrated that in medium-diameter DRG cells, similar long-duration potentials evoked

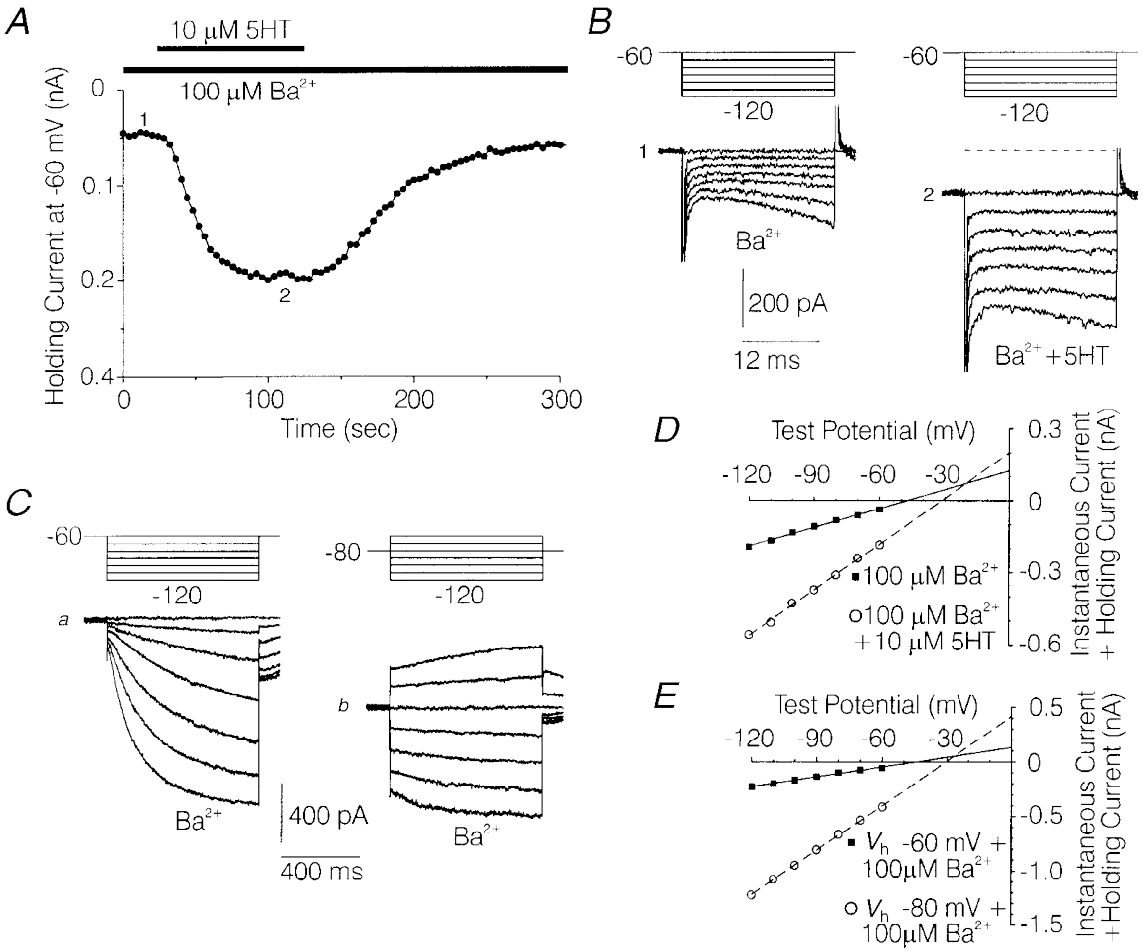

Figure 8. Determination of reversal potentials for the fast current increased by 5-HT or hyperpolarization in the presence of 100 μM Ba^{2+}

A, effect of 10 μM 5-HT on holding current at a holding potential (V_h) of −60 mV in the presence of 100 μM Ba^{2+} in a medium-diameter DRG cell. *B*, families of current sweeps taken from the experiment depicted in *A*, in the presence of 100 μM Ba^{2+} (1) and during the peak effect of 10 μM 5-HT in 100 μM Ba^{2+} (2). Each family consists of a series of 22 ms hyperpolarizations ranging from −70 to −120 mV from a V_h of −60 mV. The numbers show where the traces were taken from in *A*. *C*, families of currents evoked in the same cell as depicted in *A*, using 787 ms hyperpolarizing commands ranging from −70 to −120 mV from a V_h of −60 mV (*a*) and −80 mV (*b*), in the presence of 100 μM Ba^{2+}. *D*, plot of fast current amplitude *versus* command voltage for the currents shown in *B*1 and 2. ■, 100 μM Ba^{2+} (1). ○, 100 μM Ba^{2+} + 10 μM 5-HT (2). Straight lines were fitted to the data points using the best fit values for slope and intercept determined by linear regression. The theoretical reversal potential for the 5-HT-increased fast current, indicated by the intersection of the 2 lines, was extrapolated to be −20 mV. *E*, plot of fast current amplitude *vs.* command voltage for the currents shown in *Ca* and *b*. ■, $V_h = -60$ mV, +100 μM Ba (*a*). ○, $V_h = -80$ mV, +100 μM Ba (*b*). Straight lines were fitted to the data points for V_h values of −60 as described for *D*. The theoretical reversal potential for the hyperpolarization increased fast current was −26 mV, as estimated from straight lines fitted to the data. Fast current amplitude was measured as described in Fig. 7. Solutions were the same as those used to record I_H in Fig. 2.

by depolarizing current injection are mediated by Ca^{2+} influx through T-type Ca^{2+} channels (White *et al.* 1989; Scroggs *et al.* 1994). As mentioned above, the hyperpolarizing current pulse was adjusted to near-threshold amplitude for each cell so that anode-break consistently evoked a long-duration depolarization under control conditions (Fig. 9*Ba*). Under control conditions the long-duration depolarization consistently gave rise to one large spike and, in some cells, a second much smaller spike (Fig. 9*Ba*).

During the 5-HT-induced depolarization of the resting membrane potential, there was a reversible decrease in the amplitude of the long-duration potential evoked by anode break and in four of the five cells studied, the anode-break protocol failed intermittently to generate a long-duration depolarization (Fig. 9*Ba–c*). Complete failure of the long-duration depolarization was consistently observed upon hyperpolarization of the five cells to their respective control membrane potentials (Fig. 9*Bb*). However, regarding those cases where anode-break did evoke a long-duration depolarization while the five cells were depolarized by 5-HT, the second spike arising from the long-duration depolarization was significantly increased in amplitude by 5-HT (Fig. 9*Bb*). In the five cells studied, the second spike averaged 9 ± 3 mV under control conditions and was

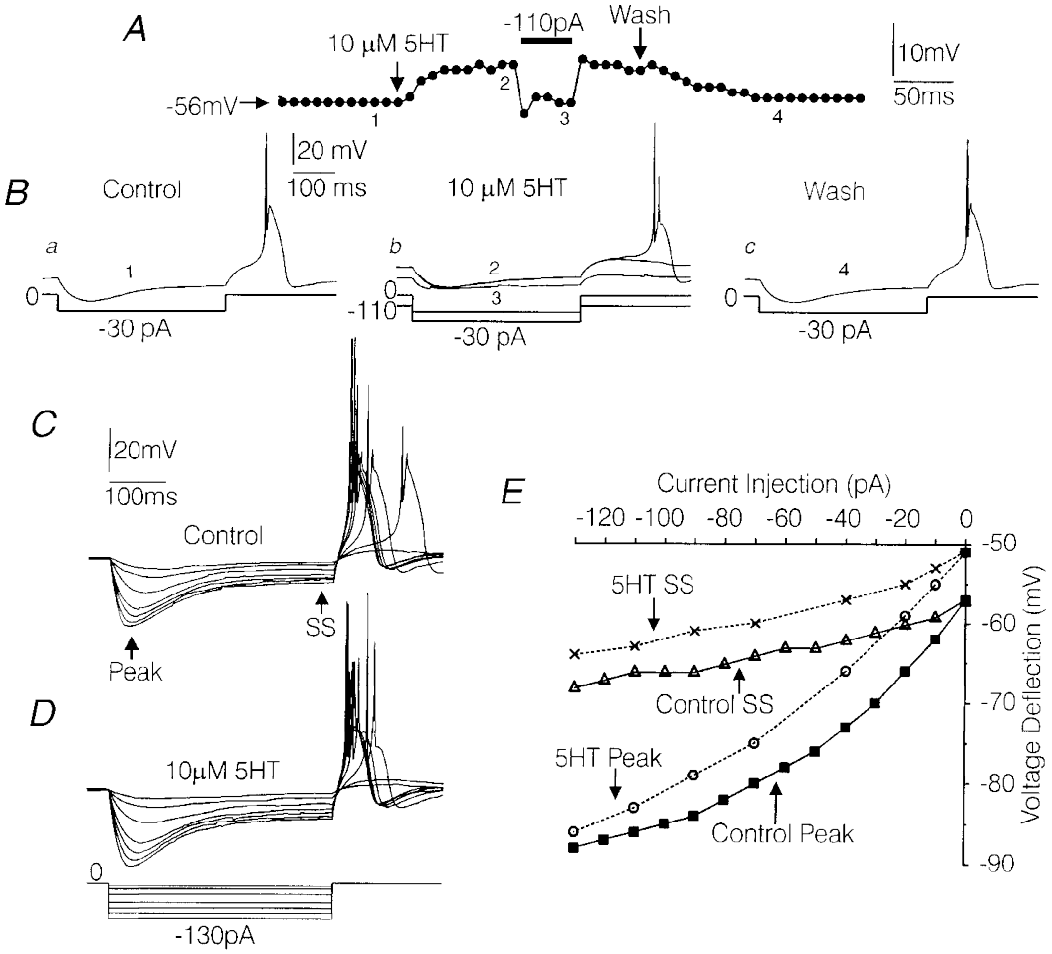

Figure 9. Effects of 5-HT on resting membrane potential, input resistance and anode-break excitation recorded in current clamp mode using patch electrodes

A, graph of resting membrane potential measured at 10 s intervals (●). During the 5-HT-induced depolarization, 110 pA of hyperpolarizing current was temporarily injected to bring the membrane potential to control levels. *B*, voltage traces showing the effects of 5-HT on input resistance and anode-break firing, in the same cell depicted in *A*, under control conditions (*a*1), during the peak effect of 5-HT (*b*2), during the injection of hyperpolarizing current (*b*3) and after washout of the effects of 5-HT (*c*4). Prior to the addition of 5-HT, the amplitude of 395 ms hyperpolarizing current pulses (given every 10 s) was adjusted to slightly past threshold as described in the text. The numbers illustrate from where in *A* the sweeps were taken from. *C–E*, study of the effects of 5-HT on the *I–V* relationship in another medium-diameter DRG cell. A series of 395 ms hyperpolarizing current pulses were delivered under control conditions (*C*) and during the peak effect of 5-HT (*D*). The resultant voltage deflections were measured at their peak and after the time-dependent rectification had reached near steady-state (SS) as indicated by the arrows. The *I–V* relationships are plotted in *E*. Solutions were the same as those used to record I_H in Fig. 2.

increased to 35 ± 7 mV during the peak effect of 5-HT ($P < 0{\cdot}05$, Wilcoxon signed-rank test). After washout of the effects of 5-HT on membrane potential, the amplitude of the second spike returned to near control levels (13 ± 4 mV) (Fig. 9*Bc*).

Figure 9*C* illustrates a current–voltage relationship constructed from one of the above-mentioned medium-diameter DRG cells in the absence and presence of 5-HT. Over most of the voltage range studied, the current–voltage relationship observed under control conditions was relatively parallel with that observed when the cell was depolarized in the presence of 5-HT (Fig. 9*E*). However, note that at later time points in the voltage sweeps (control and in the presence of 5-HT), when the voltage deflections had reached near steady-state levels, the magnitude of the voltage deflections was greatly attenuated over the entire range of currents injected (Fig. 9*C* and *D*). In contrast, at earlier time points, where the peak deflections were observed, the greatest attenuation preferentially occurred at the more negative potentials (Fig. 9*C* and *D*). This pattern was most probably produced by differences in the time course and threshold of activation of I_H *versus* I_{IR}. I_H activates more slowly and at more positive voltages relative to I_{IR} and thus probably produced the time-dependent rectification observed later in the voltage sweeps. The rectification observed at more negative membrane potentials early in the voltage sweeps was probably produced by activation of I_{IR}, which activates rapidly but at more negative membrane potentials than I_H.

DISCUSSION

The data presented indicate that in certain subpopulations of rat DRG cell bodies, 5-HT_7 and/or 5-HT_{1D} receptors are positively coupled to I_H. The idea that the 5-HT receptor involved is coupled selectively to I_H is supported by the observation that Cs^+, but not Ba^{2+}, significantly occluded the effects of 5-HT on the slow current, holding current, and fast current. In addition, the reversal potential for the 5-HT-sensitive portion of the fast current (~−23 mV) was nearly identical to the reversal potential determined for the portion of the fast current that was tonically activated by changing the holding potential from −60 to −80 mV in the presence of Ba^{2+} and thus predominantly reflects an increase in tonically activated I_H (Mayer & Westbrook, 1983). The possibility that 5-HT affected that portion of the fast current resistant to blockade by Cs^+ is argued against by the nearly complete (~98%) occlusion by Cs^+ of the effect of 5-HT on fast current.

The pharmacological profile of the receptor involved is consistent with that of the 5-HT_7 receptor, but inconsistent with that of most other 5-HT receptor subtypes. Of the 5-HT receptor types that can be demonstrated in rat DRGs (Pierce *et al.* 1996; Cardenas *et al.* 1997*a*,*b*), spiperone has a $pK_i > 6$ for 5-HT_{1A}, 5-HT_{1D}, 5-HT_{2A} and 5-HT_7 receptors, but a $pK_i < 5$ or 6 for 5-HT_{1B}, 5-HT_{1E}, 5-HT_{1F}, 5-HT_3, 5-HT_4, 5-HT_5 and 5-HT_6 receptors. Thus a 1 μM concentration of spiperone would not be expected to potently antagonize the effects of 5-HT in the latter group of 5-HT receptors (Boess & Martin, 1994; Hoyer *et al.* 1994). Of those receptors potently blocked by 1 μM spiperone, the 5-HT_{1A} receptor is an unlikely candidate, based on the lack of antagonism of the effects of 1 μM 5-HT by 1 μM cyanopindolol and the observation that the 5-HT_{1A} agonist 8-OH-DPAT did not mimic the effects of 5-HT (Boess & Martin, 1994; Hoyer *et al.* 1994). The 5-HT_{2A} receptor is also an unlikely candidate, based on the potent agonist action of 5-CT (Boess & Martin, 1994; Hoyer *et al.* 1994). 5-HT_{2C} and 5-HT_{2B} receptors have a fairly high affinity for spiperone and/or 5-CT in some assays (Hoyer, 1988; Boess & Martin, 1994) but in this study, mRNA for 5-HT_{2C} receptors could not be detected in medium-diameter DRG cells using RT-PCR and mRNA for 5-HT_{2B} receptors was not detected in whole rat DRGs with PCR in a previous study (Pierce *et al.* 1996).

Our PCR experiments did, however, demonstrate mRNA for 5-HT_7 receptors and 5-HT_{1D} receptors in most medium-diameter DRG cells tested, although the RT-PCR method does not confirm the expression of these receptors. Our PCR results are in agreement with the Pierce *et al.* (1996) study which demonstrated 5-HT_7 and 5-HT_{1D} receptor mRNA in whole rat DRGs. The rat variety of the 5-HT_{1D} receptor differs pharmacologically from its counterpart in non-rodent species and is difficult to differentiate from the 5-HT_7 receptor due to overlap in the affinities of many ligands for the two receptors. Also, there is little functional data regarding the rat 5-HT_{1D} receptor. The observation that 1 μM cyanopindolol had no agonist action with regard to the modulation of I_H in medium-diameter DRG cells could be interpreted as a lack of involvement of the 5-HT_{1D} receptor. Cyanopindolol has been shown to possess full agonist activity at non-rodent 5-HT_{1D} receptors in functional assays and has a high affinity ($pK_i = 7{\cdot}2$) for rat 5-HT_{1D} receptors (Schoeffter *et al.* 1988; Boess & Martin, 1994). However, we have not been able to find any data on the agonist activity of cyanopindolol at the rat variety of the 5-HT_{1D} receptor. There is a similar lack of direct functional evidence for other potentially useful 5-HT_{1D} agonists such as sumatriptan.

On the other hand, data regarding I_H-coupled 5-HT receptors in various neuronal types favours the idea that the 5-HT_7 receptor mediates the increase in I_H in rat DRG cells. 5-HT has been shown to increase I_H in guinea-pig thalamic and prepositus hypoglossi neurons (Pape & McCormick, 1989; Bobker & Williams, 1990). The rat brainstem as well as the guinea-pig (and rat) thalamus are rich in 5-HT_7 receptors (Ruat *et al.* 1993; Tsou *et al.* 1994; To *et al.* 1995), while 5-HT_{1D} receptor mRNA is only weakly expressed in the rat prepositus hypoglossal nucleus (Bruinvels *et al.* 1994). Thus, it is more likely that the increase in I_H produced by 5-HT in these structures is mediated by a 5-HT_7 receptor *versus* the 5-HT_{1D} receptor. In addition, the 5-HT receptor coupled to I_H in guinea-pig prepositus hypoglossi neurons responded to spiperone, 5-CT and 8-OH-DPAT with a

pattern similar to that observed for the 5-HT receptor when mediating an increase in I_H in medium-diameter rat DRG cells (Bobker & Williams, 1990), which is consistent with the pattern of affinities of these compounds at the 5-HT_7 receptor.

Our data showing that forskolin mimics and occludes the effects of 5-HT in medium-diameter DRG cells is also consistent with the idea that 5-HT_7 receptors mediate the 5-HT-induced increase in I_H. 5-HT_7 receptors have been shown to couple positively to adenylyl cyclase (Boess & Martin, 1994; Eglen *et al.* 1997). Also, several previous studies have demonstrated that enhancement of I_H involves an increase in cAMP in various neuronal types, including rat prepositus hypoglossal neurons, guinea-pig thalamic neurons and cultured mouse DRG neurons (Pape & McCormick, 1989; Bobker & Williams, 1990; Ingram & Williams, 1996; Pape, 1996; Raes *et al.* 1997). The observation that 5-HT and forskolin produce a positive shift in the conductance–voltage relationship of I_H without increasing the maximal conductance in medium-diameter DRG cells also fits with the involvement of the 5-HT_7 receptor. Several reports suggest that cAMP can bind directly to I_H channels and shift the conductance–voltage relationship without increasing the maximal conductance (Raes *et al.* 1997; Ludwig *et al.* 1998).

In contrast, numerous studies in several species have demonstrated that the 5-HT_{1D} receptor is negatively coupled to adenylyl cyclase and functions as an inhibitory presynaptic autoreceptor and/or heteroreceptor (Molderings *et al.* 1990; Waeber *et al.* 1990; Limberger *et al.* 1991; Hamblin *et al.* 1992; Boess & Martin, 1994; Bruinvels *et al.* 1994). The typical inhibitory role of the 5-HT_{1D} receptor is inconsistent with the excitatory effects associated with enhancement of I_H (Pape & McCormick, 1989; Bobker & Williams, 1990; Foehring & Waters, 1991; Pape, 1996; Yagi *et al.* 1998). Thus, the available data favours the idea that 5-HT_7 receptors, rather than 5-HT_{1D} receptors, mediate the 5-HT-induced increases in I_H observed in the neuronal types studied to date.

Enhancement of I_H has been shown to increase neuronal excitability and responsiveness to excitatory input by releasing neurons from tonic hyperpolarizing synaptic input, as well as facilitating the triggering of action potentials by depolarizing input, anode-break or counter-balancing after-hyperpolarizations following action potentials (Mayer & Westbrook, 1983; Bobker & Williams, 1989; Pape & McCormick, 1989; Foehring & Waters, 1991; Akopian & Witkovsky, 1996; Pape, 1996; Yagi *et al.* 1998). As in the above-cited cases, the enhancement of I_H by 5-HT in medium-diameter DRG cells appeared to have an overall excitatory effect. The depolarization of the resting membrane potential induced by 5-HT was not accompanied by a large decrease in input resistance, as might be expected if the depolarization was the result of an increase in tonic I_H. However, the lack of a large change in input resistance could be explained if the depolarization produced by 5-HT shut off most of the I_H channels which were tonically activated by 5-HT at the original membrane potential. The maintenance of the original input resistance would enhance the excitability of the DRG cell by preventing a large decrease in the electrotonic distance within the cell. Although 5-HT produced a more frequent failure of firing triggered by anode break when the stimulus was set close to threshold, there was a significant facilitation of a second spike in the presence of 5-HT. It seems likely that if the stimulus was sufficiently above threshold, 5-HT would have produced an overall increase in the number of action potentials triggered by anode break. Although the above data was collected in medium-diameter DRG cells which have large T-type Ca^{2+} currents, it is likely that enhancement of I_H would also increase excitability in large-diameter DRG cells, which usually lack significant T-type Ca^{2+} currents (Scroggs & Fox, 1992). A previous study demonstrated that increased activation of I_H is associated with an increase in the number of action potentials fired over the course of a depolarizing current pulse in rat DRG cells which lack large T-type Ca^{2+} currents (Yagi *et al.* 1998).

There is growing evidence that, regarding the effects of 5-HT, some characteristics of DRG cell bodies may be shared by their afferent terminals or peripheral receptors. For example, 5-HT has been demonstrated to produce a marked inhibition of high-threshold Ca^{2+} currents in C-like DRG cell bodies (Cardenas *et al.* 1995, 1997*b*). In concordance with this, other studies have demonstrated that 5-HT reduces neurotransmitter release from primary afferents terminating in the superficial dorsal horn and the spinal trigeminal nucleus, where mostly nociceptors terminate (Hori *et al.* 1996; Travagli & Williams, 1996). Furthermore, a recent finding that 5-HT produces an increase in Na^+ currents in another type of C-like DRG cell body appears relevant to the effects of 5-HT on nociceptor endings in the periphery (Cardenas *et al.* 1997*a*). Serotonin released into injured tissues by blood platelets is thought to be involved in the production of hyperalgesia, which could be explained in part by an increase in available Na^+ current in nociceptor endings (Cooper & Seesle, 1992; Taiwo & Levine, 1992).

Given the above, it is also possible that the modulation of I_H by 5-HT observed in DRG cell bodies is relevant to the effects of 5-HT at the afferent terminals or peripheral sensory receptors of the corresponding sensory neurons. For example, if I_H sensitive to 5-HT is expressed in the peripheral sensory receptors of sensory neurons corresponding to medium- and large-diameter DRG cell bodies, it is possible that 5-HT released into injured tissues might decrease the threshold for excitation. Another possibility is that 5-HT-sensitive I_H is expressed in the afferent terminals of the corresponding sensory neurons. In this case 5-HT released into the spinal cord from projections of the dorsal raphe could depolarize the terminals and facilitate neurotransmitter release. It is also possible that 5-HT may come into contact with the DRG cells themselves

as a result of nerve damage and inflammation in the vicinity of the spinal column. In this case, 5-HT may play a role in the ectopic spontaneous discharges of DRG cells associated with peripheral nerve injury (Wall & Devor, 1983; Burchiel, 1984; Kajander *et al.* 1992; Peterson *et al.* 1996).

The overall effects of 5-HT on the transmission of sensory information are likely to be quite complicated. This study has demonstrated that 5-HT enhances I_H in type 4 DRG cells and in a subpopulation of large-diameter DRG cells, but not in type 1, 2, or 3 DRG cells. Also, 5-HT has been shown to increase Na^+ currents selectively in type 2 DRG cells and inhibit Ca^{2+} currents selectively in type 1 DRG cells (Cardenas *et al.* 1995, 1997*a*,*b*). These various categories of DRG cells probably represent different types of sensory neurons. Type 1 and 2 DRG cells are capsaicin sensitive, express little or no I_H and have TTX-resistant Na^+ currents, while type 3 and 4 DRG cells and large-diameter DRG cells express prominent I_H, are capsaicin insensitive and have TTX-sensitive Na^+ currents. (Harper & Lawson, 1985*a*,*b*; Scroggs *et al.* 1994; Valiere & McLachlan, 1996). Capsaicin sensitivity, paucity of I_H and TTX-resistant Na^+ currents are typical of nociceptors, while capsaicin insensitivity, prominent I_H and TTX-sensitive Na^+ currents are typical of sensory neurons that transmit tactile and proprioceptive information (Yaksh & Hammond, 1982; Holzer, 1991; Fyffe, 1993). In addition, DRG cell body size, which varies significantly among the above-mentioned DRG cell categories, is correlated with different axonal conduction velocities (Harper & Lawson, 1985*a*,*b*) and thus may also be correlated with different types of sensory information (Yaksh & Hammond, 1982; Holzer, 1991; Fyffe, 1993). Therefore the release of 5-HT into the spinal cord or injured tissues in the periphery may simultaneously and differentially modulate several sensory modalities.

Akopian, A. & Witkovsky, P. (1996). D2 dopamine receptor-mediated inhibition of a hyperpolarization-activated current in rod photoreceptors. *Journal of Neurophysiology* **76**, 1828–1835.

Banks, M. I., Pearce, R. A. & Smith, P. H. (1993). Hyperpolarization-activated cation current (I_h) in neurons of the medial nucleus of the trapezoid body: Voltage-clamp analysis and enhancement by norepinephrine and cAMP suggest a modulatory mechanism in the auditory brain stem. *Journal of Neurophysiology* **70**, 1420–1432.

Bobker, D. H. & Williams, J. T. (1989). Serotonin augments the cationic current I_h in central neurons. *Neuron* **2**, 1535–1540.

Boess, F. G. & Martin, I. L. (1994). Molecular biology of 5-HT receptors. *Neuropharmacology* **33**, 275–317.

Bruinvels, A. T., Landwehrmeyer, B., Gustafson, E. L., Durkin, M. M., Mengod, G., Branchek, T. A., Hoyer, D. & Palacios, J. M. (1994). Localization of 5-HT_{1B}, 5-$HT_{1D\alpha}$, 5-HT_{1E}, and 5-HT_{1F} receptor messenger RNA in rodent and primate brain. *Neuropharmacology* **33**, 367–386.

Burchiel, K. J. (1984). Spontaneous impulse generation in normal and denervated dorsal root ganglia: sensitivity to alpha-adrenergic stimulation and hypoxia. *Experimental Neurology* **85**, 257–272.

Cardenas, C. G., Del Mar, L. P., Cooper, B. Y. & Scroggs, R. S. (1997*a*). $5HT_4$ receptors couple positively to tetrodotoxin-insensitive sodium channels in a subpopulation of capsaicin sensitive rat sensory neurons. *Journal of Neuroscience* **17**, 7181–7189.

Cardenas, C. G., Del Mar, L. P. & Scroggs, R. S. (1995). Variation of serotonergic inhibition of calcium channel currents in four types of rat sensory neurons differentiated by membrane properties. *Journal of Neurophysiology* **74**, 1870–1879.

Cardenas, C. G., Del Mar, L. P. & Scroggs, R. S. (1997*b*). Two parallel signaling pathways couple $5HT_{1A}$ receptors to N- and L-type Ca^{2+} channels in C-like rat dorsal root ganglion cell bodies. *Journal of Neurophysiology* **77**, 3284–3296.

Cooper, B. Y. & Sessle, B. J. (1992). Anatomy, physiology, and pathophysiology of the trigeminal system and its relationship to the development and maintenance of paraesthesies, dysesthesias, and chronic pain. In *Clinics of North America*, ed. Grigg, J. & LaBanc, J., pp. 297–332. W. B. Saunders, New York.

Eglen, R. M., Jasper, J. R., Chang, D. J. & Martin, G. R. (1997). The 5-HT_7 receptor: orphan found. *Trends in Pharmacological Sciences* **18**, 104–107.

Fyffe, R. E. W. (1983). Afferent fibers. In *Handbook of the Spinal Cord*, vol. 2 and 3, *Anatomy and Physiology*, ed. Davidoff, R. A., pp. 79–136. Marcel Dekker, New York.

Foehring, R. C. & Waters, R. S. (1991). Contributions of low-threshold calcium current and anomalous rectifier (I_h) to slow depolarizations underlying burst firing in human neocortical neurons *in vitro*. *Neuroscience Letters* **124**, 17–21.

Gold, M. S., Shuster, M. J. & Levine, J. D. (1996). Characterization of six voltage-gated K^+ currents in adult rat sensory neurons. *Journal of Neurophysiology* **75**, 2629–2646.

Hamblin, M. W., McGuffin, R. W., Metcalf, M. A., Dorsa, D. M. & Merchant, K. M. (1992). Distinct 5-HT_{1B} and 5-HT_{1D} serotonin receptors in rat: structural and pharmacological comparison of the two cloned receptors. *Molecular and Cellular Neuroscience* **3**, 578–587.

Harper, A. A. & Lawson, S. N. (1985*a*). Conduction velocity is related to morphological cell type in rat dorsal root ganglion neurones. *Journal of Physiology* **359**, 31–46.

Harper, A. A. & Lawson, S. N. (1985*b*). Electrical properties of rat dorsal root ganglion neurons with different peripheral nerve conduction velocities. *Journal of Physiology* **359**, 47–63.

Holzer, P. (1991). Capsaicin: Cellular targets, mechanisms of action, and selectivity for thin sensory neurons. *Pharmacological Reviews* **43**, 143–201.

Hori, Y., Endo, K. & Takahashi, T. (1996). Long-lasting synaptic facilitation induced by serotonin in superficial dorsal horn neurons of the rat spinal cord. *Journal of Physiology* **492**, 867–876.

Hoyer, D. (1988). Molecular pharmacology and biology of $5HT_{1C}$ receptors. *Trends in Pharmacological Sciences* **9**, 89–94.

Hoyer, D., Clarke, D. E., Fozard, J. R., Hartig, P. R., Martin, G. R., Mylecharane, E. J., Saxena, P. R. & Humphrey, P. A. (1994). International Union of Pharmacology classification of receptors for 5-hydroxytryptamine (Serotonin). *Pharmacological Reviews* **46**, 157–203.

Ingram, S. L. & Williams, J. T. (1994). Opioid inhibition of I_h via adenylyl cyclase. *Neuron* **13**, 179–186.

Ingram, S. L. & Williams, J. T. (1996). Modulation of the hyperpolarization-activated current (I_h) by cyclic nucleotides in guinea-pig primary afferent neurons. *Journal of Physiology* **492**, 97–106.

Kajander, K. C., Wakisaka, S. & Bennett, G. J. (1992). Spontaneous discharge originates in the dorsal root ganglia at the onset of a painful peripheral neuropathy in the rat. *Neuroscience Letters* **138**, 225–228.

Limberger, N., Deicher, R. & Starke, K. (1991). Species differences in presynaptic serotonin autoreceptors: mainly 5-HT_{1B} but possibly in addition 5-HT_{1D} in the rat, $5HT_{1D}$ in the rabbit and guinea-pig brain cortex. *Naunyn-Schmiedeberg's Archives of Pharmacology* **343**, 353–364.

Ludwig, A, Zong, X., Jedlitsch, M., Hoffmann, F. & Biel, M. (1998). A family of hyperpolarization-activated mammalian cation channels. *Nature* **393**, 587–591.

Mayer, M. L. & Westbrook, G. L. (1983). A voltage-clamp analysis of inward (anomalous) rectification in mouse spinal sensory ganglion neurones. *Journal of Physiology* **340**, 19–45.

Molderings, G. L., Werner, K., Likungu, J. & Gothert, M. (1990). Inhibition of noradrenaline release from the sympathetic nerves of the human saphenous vein via presynaptic 5-HT receptors similar to the 5-HT_{1D} type. *Naunyn-Schmiedeberg's Archives of Pharmacology* **342**, 371–377.

Pape, H. (1996). Queer current and pacemaker: the hyperpolarization-activated cation current in neurons. *Annual Review of Physiology* **58**, 299–327.

Pape, H. & McCormick, D. A. (1989). Noradrenaline and serotonin selectively modulate thalamic burst firing by enhancing a hyperpolarization-activated cation current. *Nature* **340**, 715–718.

Peterson, M., Zhang, J., Zhang, J.-M. & LaMotte, R. H. (1996). Abnormal spontaneous activity and responses to norepinephrine in dissociated dorsal root ganglion cells after chronic nerve constriction. *Pain* **67**, 391–397.

Pierce, P. A., Xie, G. X., Levine, J. D. & Peroutka, S. J. (1996). 5-Hydroxytryptamine receptor subtype messenger RNAs in rat peripheral sensory and sympathetic ganglia: a polymerase chain reaction study. *Neuroscience* **70**, 553–559.

Raes, A., Wang, Z., Van den Berg, R. J., Goethals, M., Van de Vijver, G. & Van Boggaert, P. P. (1997). Effect of cAMP and ATP on the hyperpolarization-activated current in mouse dorsal root ganglion neurons. *Pflügers Archiv* **434**, 543–550.

Ruat, M., Traiffort, E., Leurs, R., Tardivel-Lacombe, J., Diaz, J., Arrang, J. & Schwartz, J. (1993). Molecular cloning, characterization, and localization of a high-affinity serotonin receptor ($5HT_7$) activating cAMP formation. *Proceedings of the National Academy of Sciences of the USA* **90,** 8547–8551.

Schoeffter, P., Waeber, C., Palacios, J. M. & Hoyer, D. (1988). The 5-hydroxytryptamine 5-HT_{1D} receptor subtype is negatively coupled to adenylate cyclase in calf substantia nigra. *Naunyn-Schmiedeberg's Archives of Pharmacology* **337**, 602–608.

Scroggs, R. S. & Fox, A. P. (1992). Calcium current variation between acutely isolated adult rat dorsal root ganglion neurons of different size. *Journal of Physiology* **445**, 639–658.

Scroggs, R. S., Todorovic, S., Anderson, E. G. & Fox, A. P. (1994). Variation in I_H, I_{IR}, and I_{LEAK} between acutely isolated adult rat dorsal root ganglion neurons of different size. *Journal of Neurophysiology* **71**, 271–279.

Taiwo, Y. O. & Levine, J. D. (1992). Serotonin is a directly-acting hyperalgesic agent in the rat. *Neuroscience* **48**, 485–490.

To, Z. P., Bonhaus, D. W., Eglen, R. M. & Jakeman, L. B. (1995). Characterization and distribution of putative 5-ht_7 receptors in guinea-pig brain. *British Journal of Pharmacology* **115**, 107–116.

Travagli, R. A. & Williams, J. T. (1996). Endogenous monoamines inhibit glutamate transmission in the spinal trigeminal nucleus of the guinea-pig. *Journal of Physiology* **491**, 177–185.

Tsou, A., Kosaka, A., Bach, C., Zuppan, P., Yee, C., Tom, L., Alvarez, R., Ramsey, S., Bonhaus, W., Stefanich, E., Jakeman, L., Eglen, M. & Chan, H. W. (1994). Cloning and expression of a 5-hydroxytryptamine$_7$ receptor positively coupled to adenyl cyclase. *Journal of Neurochemistry* **63**, 456–464.

Villiere, V. & McLachlan, E. M. (1996). Electrophysiological properties of neurons in intact rat dorsal root ganglia classified by conduction velocity and action potential duration. *Journal of Neurophysiology* **76**, 1924–1941.

Waeber, C., Schoeffter, P., Hoyer, D. & Palacios, J. M. (1990). The serotonin 5-HT_{1D} receptor: a progress review. *Neurochemical Research* **15**, 567–582.

Wall, P. D. & Devor, M. (1983). Sensory afferent impulses originate from dorsal root ganglia as well as from the periphery in normal and nerve injured rats. *Pain* **17,** 321–339.

White, G., Lovinger, D. M. & Weight, F. F. (1989). Transient low threshold Ca^{2+} current triggers burst firing through an afterdepolarizating potential in an adult mammalian neuron. *Proceedings of the National Academy of Sciences of the USA* **86**, 6802–6806.

Yagi, J., Yamaguchi, K. & Sumino, R. (1998). Inhibition of a hyperpolarization-activated current by clonidine in rat dorsal root ganglion neurons. *Journal of Neurophysiology* **80**, 1094–1104.

Yaksh, T. L. & Hammond, D. L. (1982). Peripheral and central substrates involved in the rostrad transmission of nociceptive information. *Pain* **13,** 1–85.

Acknowledgements

This work was supported by National Science Foundation grant IBN-9310065 and NIH grant NS37067 awarded to R. S. Scroggs and NIH grant NS 36496 to D. J. Surmeier.

Corresponding author

R. S. Scroggs: Department of Anatomy and Neurobiology, College of Medicine, University of Tennessee, Memphis, TN 38163, USA.